LOOPE: Learnable Optimal Patch Order for Positional Encoders in Vision Transformers (Supplementary Material)

Anonymous CVPR: 2026 submission

A Methodology

A.1 Gilbert Curve Generation (Generalized Hilbert Curve)

The following pseudocode represents a recursive algorithm for generating a generalized Hilbert (Gilbert) space-filling curve for arbitrary 2D rectangular grids. The algorithm outputs discrete 2D coordinates that fill a rectangle of given width and height.

A.1.1 Main Procedure: `gilbert2d`

Algorithm 1 `gilbert2d(width, height)`

```
function GILBERT2D($width$, $height$)
    if $width \geq height$ then
        return GENERATE2D(0, 0, $width$, 0, 0, $height$)
    else
        return GENERATE2D(0, 0, 0, $height$, $width$, 0)
```

A.1.2 Helper Function: `sgn`

Algorithm 2 `sgn(x)`

```
function SGN($x$)
    if $x < 0$ then
        return $-1$
    else if $x > 0$ then
        return 1
    else
        return 0
```

A.1.3 Recursive Procedure: `generate2d`

Algorithm 3 `generate2d(x, y, ax, ay, bx, by)`

```
procedure GENERATE2D($x, y, ax, ay, bx, by$)
    $w \leftarrow |ax + ay|$                                ▷ Effective width
    $h \leftarrow |bx + by|$                                ▷ Effective height
    $(dax,\ day) \leftarrow (\text{sgn}(ax),\ \text{sgn}(ay))$    ▷ Unit vector in major direction
    $(dbx,\ dby) \leftarrow (\text{sgn}(bx),\ \text{sgn}(by))$    ▷ Unit vector in orthogonal direction
    if $h = 1$ then
        for $i \leftarrow 0$ to $w - 1$ do
            Output $(x, y)$
            $(x, y) \leftarrow (x + dax,\ y + day)$
        return
    if $w = 1$ then
        for $i \leftarrow 0$ to $h - 1$ do
            Output $(x, y)$
            $(x, y) \leftarrow (x + dbx,\ y + dby)$
        return
    $(ax2,\ ay2) \leftarrow (\lfloor ax/2 \rfloor,\ \lfloor ay/2 \rfloor)$
    $(bx2,\ by2) \leftarrow (\lfloor bx/2 \rfloor,\ \lfloor by/2 \rfloor)$
    $w2 \leftarrow |ax2 + ay2|$
    $h2 \leftarrow |bx2 + by2|$
    if $2w > 3h$ then                                      ▷ Long case: split into two parts
        if $(w2 \bmod 2 = 1)$ and $(w > 2)$ then
            $(ax2,\ ay2) \leftarrow (ax2 + dax,\ ay2 + day)$          ▷ Prefer even steps
        GENERATE2D($x,\ y,\ ax2,\ ay2,\ bx,\ by$)
        GENERATE2D($x + ax2,\ y + ay2,\ ax - ax2,\ ay - ay2,\ bx,\ by$)
    else
        if $(h2 \bmod 2 = 1)$ and $(h > 2)$ then
            $(bx2,\ by2) \leftarrow (bx2 + dbx,\ by2 + dby)$          ▷ Prefer even steps
        GENERATE2D($x,\ y,\ bx2,\ by2,\ ax2,\ ay2$)
        GENERATE2D($x + bx2,\ y + by2,\ ax,\ ay,\ bx - bx2,\ by - by2$)
        GENERATE2D($x + (ax - dax) + (bx2 - dbx),\ y + (ay - day) + (by2 -$
    $dby),\ -bx2,\ -by2,\ -(ax - ax2),\ -(ay - ay2)$)
```

Notes:

- The function `gilbert2d` selects the major direction based on the aspect ratio.
- The helper function `sgn` returns the sign of its input.
- The `generate2d` procedure is recursive. It subdivides the rectangle until reaching trivial row or column fills, outputting coordinate points at each base case.

- In this pseudocode, "**Output** (x, y)" corresponds to yielding the coordinate in the Python implementation.

A.2 Context-Aware Index Generator Architecture

The architecture of the context-aware bias generator X_C is summarized in Table 1. The module takes as input the RGB image ($I_0 \in \mathbf{R}^{3\times H\times W}$) concatenated with coordinate maps ($x, y \in \mathbf{R}^{1\times H\times W}$), forming a 5-channel tensor. Through a series of convolutional layers followed by batch normalization, flattening, and an MLP, the network outputs continuous offsets $X_C \in \mathbf{R}^{1\times N}$, which refine the static patch order X_G.

Table 1: Layer-wise specification of the context-aware index generator for X_C. Conv$_k$ denotes a convolution with kernel size $k \times k$. All convolutions use ReLU activations unless stated otherwise.

Layer	**Input Shape**	**Operation**	**Output Shape**	**Notes**
Input	$[5 \times H \times W]$	—	$[5 \times H \times W]$	RGB + coordinate maps
Conv1	$[5 \times H \times W]$	32 filters, kernel $P \times P$, stride 16	$[32 \times h \times w]$	Downsampling to patch scale
Conv2	$[32 \times h \times w]$	16 filters, kernel 5×5, stride 1	$[16 \times h \times w]$	Local refinement
Conv3	$[16 \times h \times w]$	8 filters, kernel 5×5, stride 1	$[8 \times h \times w]$	—
Conv4	$[8 \times h \times w]$	4 filters, kernel 5×5, stride 1	$[4 \times h \times w]$	—
Conv5	$[4 \times h \times w]$	1 filter, kernel 5×5, stride 1	$[1 \times h \times w]$	Channel squeeze
BN + Flatten	$[1 \times h \times w]$	BatchNorm + reshape	$[1 \times N]$	$N = h \times w$ patches
MLP	$[1 \times N]$	Linear layer + bias	$[1 \times N]$	Fully connected refinement
Activation	$[1 \times N]$	$2\sigma(x) - 1$	$X_C \in [-1, 1]^{1\times N}$	Fractional offsets

The stride of 16 in Conv1 ensures that each feature corresponds to a patch region of the image, aligning X_C directly with the patch grid used by the transformer. Subsequent layers refine this representation without further spatial downsampling, keeping the module lightweight and efficient.

A.3 Theoretical Effect of Context-Aware Adaptation on Frequency Sensitivity

To analyze why the context-aware refinement X_C reduces sensitivity to the choice of frequency set, consider a simplified form of the positional encoding:

$$\mathrm{PE}(f) = \sin\left(\frac{(x + \delta)}{N} f\right), \tag{1}$$

where x is the static patch index, δ is the adaptive offset produced by the context-aware generator, N is the normalization factor (e.g., $N = 196$ for a 14×14 patch grid), and f is the frequency. The offset δ itself depends on both the frequency and local image context:

$$\delta = g(f, \text{context}).$$

Frequency sensitivity without adaptation. When $\delta = 0$, the derivative of PE with respect to f is

$$\frac{\partial}{\partial f}\,\mathrm{PE}(f) = \frac{x}{N}\cos\left(\frac{x}{N}f\right). \tag{2}$$

Thus, sensitivity is strictly proportional to the normalized index x/N. In this case, different choices of frequency sets directly translate into large oscillations in the embedding, making performance highly dependent on design choices.

Frequency sensitivity with adaptation. With context-aware refinement ($\delta \neq 0$), we compute

$$\begin{aligned}\frac{\partial}{\partial f}\,\mathrm{PE}(f) &= \frac{\partial}{\partial f}\,\sin\left(\frac{(x+\delta)}{N}f\right)\\ &= \cos\left(\frac{(x+\delta)}{N}f\right)\cdot\frac{\partial}{\partial f}\left(\frac{(x+\delta)}{N}f\right).\end{aligned} \tag{3}$$

Expanding the inner derivative:

$$\frac{\partial}{\partial f}\left(\frac{(x+\delta)}{N}f\right) = \frac{x+\delta}{N} + \frac{f}{N}\frac{\partial\delta}{\partial f}. \tag{4}$$

Substituting back into Eq. 3 gives the simplified expression:

$$\frac{\partial}{\partial f}\,\mathrm{PE}(f) = \left(\frac{x+\delta}{N} + \frac{f}{N}\frac{\partial\delta}{\partial f}\right)\cos\left(\frac{(x+\delta)}{N}f\right). \tag{5}$$

Interpretation. Equation 5 reveals two contributions to frequency sensitivity:

- $\frac{x+\delta}{N}$: a shifted static term, analogous to the non-adaptive case but now adjusted by the learned offset δ.
- $\frac{f}{N}\frac{\partial\delta}{\partial f}$: an adaptive correction term, which enables the model to compensate for changes in the frequency set.

Without adaptation, only the first term exists, making sensitivity rigidly determined by x/N. With adaptation, the second term actively counterbalances frequency variations, thereby reducing sensitivity while preserving the sinusoidal form of the encoding.

Conclusion. Context-aware adaptation therefore moderates the dependency on frequency selection: the encoding remains sinusoidal in structure, ensuring consistency, but the added corrective term $\frac{\partial \delta}{\partial f}$ provides robustness. This theoretical view aligns with the empirical results in Table. 7, where LOOPE maintains stable accuracy even under non-optimal frequency choices.

A.4 Three Cell experiment

Overview

This dataset is designed to facilitate research in spatial reasoning, geometric transformations, and pattern recognition using synthetic images. It consists of structured grid-based images where three distinct color markers (red, green, and blue) are positioned according to predefined spatial constraints.

Purpose & Applications

The dataset supports tasks such as:

- **Machine Learning & Deep Learning:** Training models to understand spatial relationships.
- **Computer Vision:** Evaluating geometric transformations and positional reasoning.
- **Representation Learning:** Analyzing how models interpret structured spatial layouts.

Dataset Statistics and Description

- The dataset consists of 10,000 synthetic images.
- The cell coordinates are uniformly sampled on a 14×14 grid.
- The relative cases are designed to be equiprobable, ensuring balanced distribution.
- Among the 196 patches, 193 are colored black; the three colored patches are non-colinear and non-overlapping, however they can share boundaries.

Three-Cell Experiment Dataset Visualization

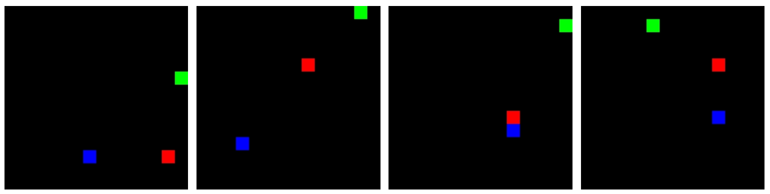

(a) (b) (c) (d)

Figure 1: Three-Cell Experiment Sample Dataset

Structure & Content Each sample includes:

1. **Image:** A 224×224 pixel RGB image that represents a 14×14 grid. In this grid:
   - A red cell serves as the reference point.
   - A green cell and a blue cell are positioned based on mathematical constraints.
   - The background is black, with each cell having a distinct color.
2. **Binary Mask:** A 6-element vector encoding specific spatial properties, such as:
   - Distance comparisons.
   - Geometric orientation.
   - Area relationships.

Key Characteristics

- **Controlled Complexity:** Images are generated based on strict mathematical rules.
- **Diversity:** Multiple spatial configurations ensure a wide range of positional relationships.
- **Explainability:** The structured nature of the dataset makes it ideal for interpretable AI research.

Potential Use Cases

- Training AI models for spatial awareness and geometric reasoning.
- Benchmarking representation learning techniques in structured visual tasks.
- Investigating how neural networks learn spatial relationships in a controlled setting.

Algorithm 4 Synthetic Image Dataset Generation

```
1: **procedure** GenerateSyntheticDataset
2:     **Input:** Grid size $G \leftarrow 14$, Sum-of-squares limit $L \leftarrow 338$, $max\_attempts$
3:     **Output:** Expanded grid image $grid_{224}$ and binary mask $mask[6]$
4:     $max\_val \leftarrow \lfloor \sqrt{L} \rfloor$
5:     Initialize dictionary $D \leftarrow \emptyset$
6:     **for** $a = -max\_val$ **to** $max\_val$ **do**
7:         **for** $b = -max\_val$ **to** $max\_val$ **do**
8:             $n \leftarrow a^2 + b^2$
9:             **if** $n \leq L$ **then**
10:                Append pair $(a, b)$ to $D[n]$
11:    Remove keys from $D$ that have only one representation
12:    Randomly choose mode from $\{1, 2, 3\}$
13:    $valid \leftarrow$ **false**
14:    **while** not $valid$ **do**
15:        Randomly select red cell $X_r \in [0, G-1]^2$
16:        **if** mode $= 1$ **then**
17:            Select random key $k$ from keys of $D$
18:            **for** $attempt = 1$ to $max\_attempts$ **do**
19:                Randomly choose two distinct pairs $(a_1, b_1)$ and $(a_2, b_2)$ from $D[k]$
20:                $X_g \leftarrow X_r + (a_1, b_1)$
21:                $X_b \leftarrow X_r + (a_2, b_2)$
22:                **if** $X_g$ and $X_b$ are within the grid and distinct from $X_r$ and each other **then**
23:                    $valid \leftarrow$ **true**
24:                    **break**
25:        **else if** mode $\in \{2, 3\}$ **then**
26:            **for** $attempt = 1$ to $max\_attempts$ **do**
27:                Randomly select two keys $k_1, k_2$ from $D$
28:                **if** mode $= 2$ **then**
29:                    $k_g \leftarrow \min(k_1, k_2)$, $k_b \leftarrow \max(k_1, k_2)$
30:                **else**
31:                    $k_g \leftarrow \max(k_1, k_2)$, $k_b \leftarrow \min(k_1, k_2)$
32:                Randomly select pair $(a_g, b_g)$ from $D[k_g]$ and $(a_b, b_b)$ from $D[k_b]$
33:                $X_g \leftarrow X_r + (a_g, b_g)$
34:                $X_b \leftarrow X_r + (a_b, b_b)$
35:                **if** $X_g$ and $X_b$ are within the grid and distinct **then**
36:                    $valid \leftarrow$ **true**
37:                    **break**
38:    Create a $G \times G$ grid $grid_{14}$ with black background
39:    Set $grid_{14}[X_r] \leftarrow$ red, $grid_{14}[X_g] \leftarrow$ green, $grid_{14}[X_b] \leftarrow$ blue
40:    Expand $grid_{14}$ to $grid_{224}$ by replicating each cell into a $16 \times 16$ block
41:    Initialize mask $mask[6] \leftarrow (0, 0, 0, 0, 0, 0)$
42:    **Call** sub-procedures:
         • DistanceCompare($X_r, X_g, X_b, mask$)
         • Orientation($X_r, X_g, X_b, mask$)
         • AreaCompare($X_r, X_g, X_b, mask$)
         • VectorSum($X_r, X_g, X_b, mask$)
43:    **return** $grid_{224}$ and $mask$
```

A.5 Positional Embeddings Structural Integrity (PESI) Metrics

A.5.1 Undirected Monotonicity

Algorithm 5 Compute Global Undirected Monotonicity Score M_u

```
Input: Positional embedding tensor $P \in R^{H \times W \times D}$
Output: Global undirected monotonicity score $M_u$

1: Initialize an empty list $S \leftarrow [\,]$   ▷ Will store Spearman correlations for each cell
2: for $x = 1, 2, \ldots, H$ do
3:     for $y = 1, 2, \ldots, W$ do
4:         $v_{\text{center}} \leftarrow P(x, y, :)$
5:         Compute norm: $\|v_{\text{center}}\| \leftarrow \text{norm}(v_{\text{center}}) + \epsilon$
6:         Compute cosine similarity for all $(i, j)$:
               $$A_{(x,y)}(i,j) \leftarrow \frac{v_{\text{center}} \cdot P(i,j,:)}{\|v_{\text{center}}\| \cdot \|P(i,j,:)\| + \epsilon}$$
7:         Compute Euclidean distances:
               $$d(i,j) \leftarrow \sqrt{(i-x)^2 + (j-y)^2}$$
8:         Form radial bins: $r(i,j) \leftarrow \text{round}\big(d(i,j)\big)$
9:         for each unique radial bin $r$ do
10:            $S_{(x,y)}(r) \leftarrow$ average of $A_{(x,y)}(i,j)$ for all $(i,j)$ with $r(i,j) = r$
11:        Compute Spearman's rank correlation $\rho_{(x,y)}$ between the set $\{r\}$ and $\{S_{(x,y)}(r)\}$
12:        Append $\rho_{(x,y)}$ to $S$
13: Compute global score:
        $$M_u \leftarrow \frac{1}{HW} \sum_{(x,y)} \Big(1 - \rho_{(x,y)}\Big)$$
14: return $M_u$
```

A.5.2 Directed Monotonicity

Algorithm 6 Compute Global Directed Monotonicity Measure M_D

Input: Positional embedding tensor $P \in R^{H\times W\times D}$, quantization angle δ

Output: Global directed monotonicity measure M_D

```
1: $N \leftarrow \lceil 2\pi/\delta \rceil$                                ▷ Total number of directional buckets
2: Initialize list $S \leftarrow [\,]$                                  ▷ Stores $1 - \bar{\rho}_{(x,y)}$ for each cell
3: for $x = 1, 2, \ldots, H$ do
4:     for $y = 1, 2, \ldots, W$ do
5:         $v_{\text{center}} \leftarrow P(x, y, :)$
6:         Compute cosine similarity for all cells:
               $$A_{(x,y)}(i,j) \leftarrow \frac{v_{\text{center}} \cdot P(i,j,:)}{\|v_{\text{center}}\| \, \|P(i,j,:)\| + \epsilon}$$
7:         Compute radial distances:
               $$d(i,j) \leftarrow \sqrt{(i-x)^2 + (j-y)^2}$$
8:         Compute angles:
               $$\theta_{(x,y)}(i,j) \leftarrow \operatorname{atan2}(j-y,\, i-x)$$
9:         Quantize angles into buckets:
               $$k(i,j) \leftarrow \left\lfloor \frac{\theta_{(x,y)}(i,j)}{\delta} \right\rfloor \mod N$$
10:        Initialize list $\rho^k \leftarrow [\,]$                    ▷ Bucket correlations for cell $(x,y)$
11:        for $k = 0, 1, \ldots, N-1$ do
12:            Let $B_k \leftarrow \{(i,j) \mid k(i,j) = k\}$
13:            if $|B_k| < 2$ then
14:                Append 0 to $\rho^k$
15:            else
16:                Order $B_k$ by increasing $d(i,j)$
17:                Compute similarity profile $S^k_{(x,y)}(r)$ for the ordered cells
18:                Compute Spearman's rank correlation:
                       $$\rho^k_{(x,y)} \leftarrow 1 - \frac{6\sum_r d_r^2}{|B_k|(|B_k|^2 - 1)}$$
19:                Append $\rho^k_{(x,y)}$ to $\rho^k$
20:        Compute mean correlation for cell:
               $$\bar{\rho}_{(x,y)} \leftarrow \frac{1}{N}\sum_{k=0}^{N-1} \rho^k$$
21:        Append $1 - \bar{\rho}_{(x,y)}$ to $S$
22: Compute global measure:
               $$M_D \leftarrow \frac{1}{HW}\sum_{(x,y)} \left(1 - \bar{\rho}_{(x,y)}\right)$$
23: return $M_D$
```

A.5.3 Undirected Asymmetry

Algorithm 7 Compute Global Undirected Asymmetry A_{SU}

Input: Positional embedding tensor $P \in R^{H \times W \times D}$

Output: Global undirected asymmetry measure A_{SU}

```
1: for each center $(x, y)$ in $\{1, \ldots, H\} \times \{1, \ldots, W\}$ do
2:     Compute cosine similarity:
           $$A_{(x,y)}(i,j) = \frac{P(x,y,:) \cdot P(i,j,:)}{\|P(x,y,:)\| \, \|P(i,j,:)\|}$$
3:     Compute Euclidean distance:
           $$d(i,j) = \sqrt{(i-x)^2 + (j-y)^2}$$
4:     Define radial bins:
           $$B_r = \{(i,j) \mid r = \text{round}(d(i,j))\}$$
5:     for each radial bin $r \in R$ do
6:         Compute mean similarity:
               $$\mu_{(x,y)}(r) = \frac{1}{|B_r|} \sum_{(i,j) \in B_r} A_{(x,y)}(i,j)$$
7:         Compute standard deviation:
               $$\sigma_{(x,y)}(r) = \sqrt{\frac{1}{|B_r|} \sum_{(i,j) \in B_r} \left(A_{(x,y)}(i,j) - \mu_{(x,y)}(r)\right)^2}$$
8:         Compute coefficient of variation:
               $$\text{CV}_{(x,y)}(r) = \frac{\sigma_{(x,y)}(r)}{\mu_{(x,y)}(r)}$$
9:     Compute undirected asymmetry for center $(x, y)$:
           $$A'_{SU}(x,y) = \frac{1}{|R|} \sum_{r \in R} \text{CV}_{(x,y)}(r)$$
10: Compute global asymmetry measure:
           $$A_{SU} = \frac{1}{HW} \sum_{x=1}^{H} \sum_{y=1}^{W} A'_{SU}(x,y)$$
11: return $A_{SU}$
```

A.6 Sensitivity Calculation Documentation

We consider four input signals of length $L = 768$:

$$f_1(i) = 0.978^i, \tag{6}$$

$$f_2(i) = 1 - i\frac{1 - 0.0001}{L - 1}, \tag{7}$$

$$f_3(i) = 0.9^i, \tag{8}$$

$$f_4(i) \sim \text{Uniform}(0.0001, 1), \text{sorted descending.} \tag{9}$$

The first signal f_1 is chosen as the baseline reference.

A.6.1 Relative Change of Input Signals

For each signal f_j ($j = 2, 3, 4$), its relative change compared to the baseline f_1 is computed as the normalized root mean squared difference:

$$\Delta f_j = \frac{\|f_j - f_1\|_2}{\|f_1\|_2}, \tag{10}$$

where $\|\cdot\|_2$ denotes the Euclidean norm.

A.6.2 Output Values

Each black-box algorithm produces four output values corresponding to the four input signals. Denote the outputs for algorithm k as

$$O^{(k)} = [O_1^{(k)}, O_2^{(k)}, O_3^{(k)}, O_4^{(k)}], \tag{11}$$

where $O_1^{(k)}$ is the output corresponding to the baseline f_1.

A.6.3 Sensitivity per Input

For each algorithm k and each signal $j = 2, 3, 4$, the sensitivity is defined as the ratio of the absolute output change to the relative input change:

$$S_j^{(k)} = \frac{|O_j^{(k)} - O_1^{(k)}|}{\Delta f_j}. \tag{12}$$

A.6.4 Normalized Average Sensitivity

Since the relative changes Δf_j may differ significantly across signals, we compute a normalized weighted average sensitivity for each algorithm:

$$\bar{S}^{(k)} = \frac{\sum_{j=2}^{4} S_j^{(k)} \Delta f_j}{\sum_{j=2}^{4} \Delta f_j}. \tag{13}$$

This measure reflects the overall sensitivity of the algorithm to input variations, properly weighted by the magnitude of the input changes.

B Visualization

Since, showing exactly how the properties in Table 1, retains in real-life vision tasks is quite hard and the lone contribution of PEs to the performance of ViTs are not huge (generally 4-6%). That's why generating an edge case, where any property may fail/pass, is barely possible. Instead, we can visually verify the implication of PESI metrics in the plotted correlation map of Positional encoding. In 2, it has shown the correlation map with different location of patch, on different embedding policy.

From instance, according to Table 6, LFF(fourier) have highest Directed Monotonicity, M_D, as any viewer can see, LFF has the smoothest descending correlation in any particular direction. But, LOOPE has the highest score in Undirected Monotonicity.

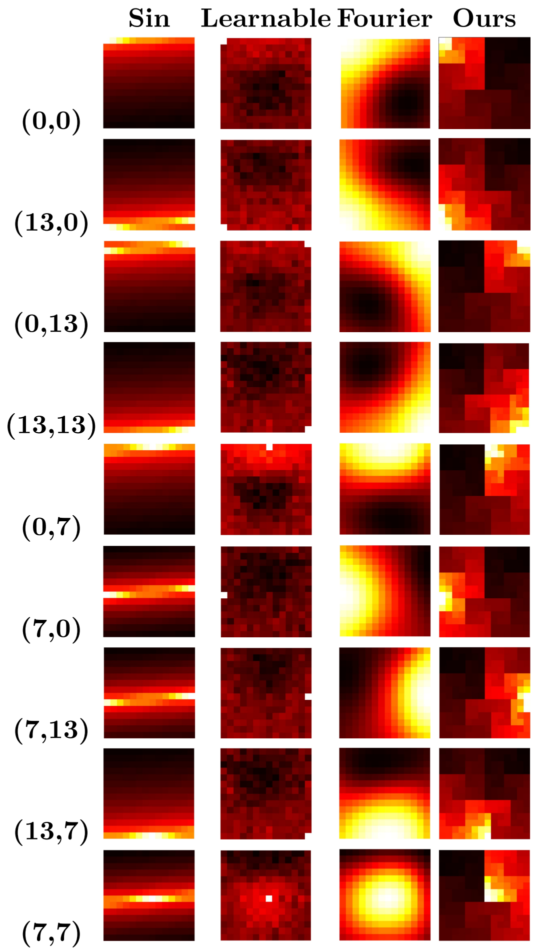

Figure 2: Cosine Similarity Map Comparison among varios PEs on different positions